

This is a copy of the published version, or version of record, available on the publisher's website. This version does not track changes, errata, or withdrawals on the publisher's site.

Understanding the role of additive manufacturing in the development of astronomical hardware

Carolyn Atkins, Younes Chahid, James T. Wells, Marcell Westsik, Katherine Morris, Ciarán Breen, Alastair Macleod, Lawrence Bissell, William Cochrane, Richard Kotlewski, Scott McPhee, Robert M. Snell, Iain Todd, Mat Beardsley, Michael Harris, Misael Pimentel, Scott McKeegney, Jonathan Orr, Simon G. Alcock, Ioana Theodora Nistea, Simone Cottarelli, and Samuel Tammam-Williams

Published version information:

Citation: Carolyn Atkins, Younes Chahid, James T. Wells, Marcell Westsik, Katherine Morris, Ciarán Breen, Alastair Macleod, Lawrence Bissell, William Cochrane, Richard Kotlewski, Scott McPhee, Robert M. Snell, Iain Todd, Mat Beardsley, Michael Harris, Misael Pimentel, Scott McKeegney, Jonathan Orr, Simon G. Alcock, Ioana Theodora Nistea, Samuel Tammam-Williams, Simone Cottarelli, "Understanding the role of additive manufacturing in the development of astronomical hardware," Proc. SPIE 12677, Astronomical Optics: Design, Manufacture, and Test of Space and Ground Systems IV, 126770L (4 October 2023)

DOI: <https://doi.org/10.1117/12.2677452>

Copyright 2023 Society of Photo-Optical Instrumentation Engineers (SPIE). One print or electronic copy may be made for personal use only. Systematic reproduction and distribution, duplication of any material in this publication for a fee or for commercial purposes, and modification of the contents of the publication are prohibited.

This version is made available in accordance with publisher policies. Please cite only the published version using the reference above. This is the citation assigned by the publisher at the time of issuing the APV. Please check the publisher's

This item was retrieved from **ePubs**, the Open Access archive of the Science and Technology Facilities Council, UK. Please contact epublications@stfc.ac.uk or go to <http://epubs.stfc.ac.uk/> for further information and policies.

PROCEEDINGS OF SPIE

SPIDigitalLibrary.org/conference-proceedings-of-spie

Understanding the role of additive manufacturing in the development of astronomical hardware

Carolyn Atkins, Younes Chahid, James Wells, Marcell Westsik, Katherine Morris, et al.

Carolyn Atkins, Younes Chahid, James T. Wells, Marcell Westsik, Katherine Morris, Ciarán Breen, Alastair Macleod, Lawrence Bissell, William Cochrane, Richard Kotlewski, Scott McPhee, Robert M. Snell, Iain Todd, Mat Beardsley, Michael Harris, Misael Pimentel, Scott McKegney, Jonathan Orr, Simon G. Alcock, Ioana Theodora Nistea, Samuel Tammas-Williams, Simone Cottarelli, "Understanding the role of additive manufacturing in the development of astronomical hardware," Proc. SPIE 12677, Astronomical Optics: Design, Manufacture, and Test of Space and Ground Systems IV, 126770L (4 October 2023); doi: 10.1117/12.2677452

SPIE.

Event: SPIE Optical Engineering + Applications, 2023, San Diego, California, United States

Understanding the role of additive manufacturing in the development of astronomical hardware

Carolyn Atkins^{a*}, Younes Chahid^a, James T. Wells^{a, b}, Marcell Westsik^{a, c}, Katherine Morris^a, Ciarán Breen^a, Alastair Macleod^a, Lawrence Bissell^a, William Cochrane^a, Richard Kotlewski^a, Scott McPhee^a, Robert M. Snell^b, Iain Todd^b, Mat Beardsley^d, Michael Harris^d, Misaël Pimentel^e, Scott McKegey^e, Jonathan Orr^e, Simon G. Alcock^f, Ioana Theodora Nistea^f, Simone Cottarelli^g, and Samuel Tammias-Williams^g

^aUK Astronomy Technology Centre, Royal Observatory, Edinburgh, EH9 3HJ, UK

^bDept of Materials Science and Engineering, University of Sheffield, Sheffield, S1 3JD, UK

^cDept of Mechanical, Aerospace & Civil Engineering, University of Manchester, M13 9PL, UK

^dRAL Space, Harwell Science & Innovation Campus, OX11 0QX, UK

^eNational Manufacturing Institute Scotland, Renfrew, PA3 2EF, UK

^fDiamond Light Source, Harwell Science & Innovation Campus, OX11 0QX, UK

^gSchool of Engineering, University of Edinburgh, Edinburgh, EH9 3FB, UK

ABSTRACT

Lightweight optical manufacture is no longer confined to the conventional subtractive (mill and drill), formative (casting and forging) and fabricative (bonding and fixing) manufacturing methods. Additive manufacturing (AM; 3D printing), creating a part layer-by-layer, provides new opportunities to reduce mass and combine multiple parts into one structure. Frequently, modern astronomical telescopes and instruments, ground- and space-based, are limited in mass and volume, and are complex to assemble, which are limitations that can benefit from AM. However, there are challenges to overcome before AM is considered a conventional method of manufacture, for example, upskilling engineers, increasing the technology readiness level via AM case studies, and understanding the AM build process to deliver the required material properties.

This paper describes current progress within a four-year research programme that has the goal to explore these challenges towards creating a strategy for AM adoption within astronomical hardware. Working with early-career engineers, case studies have been undertaken which focus on lightweight AM aluminium mirror manufacture and optical mountings. In parallel, the aluminium AM build parameters have been investigated to understand which combination of parameters results in AM parts with consistent material properties and low defects. Metrology results from two AM case studies will be summarised: the optical characteristics of a lightweighted aluminium mirror intended for in-orbit deployment from a nanosat; and the AM build quality of wire arc additive manufacture for use in an optomechanical housing. Finally, an analysis of how surface roughness from AM mirror samples and build parameters are linked will be discussed.

Keywords: Astronomical instrumentation, lightweight metal mirrors, additive manufacturing, 3D printing, design optimisation, material properties.

1. INTRODUCTION

Research-grade astronomical hardware, both telescopes and instruments, is frequently bespoke and for the ‘flagship’ projects (for example, the Extremely Large Telescope - ELT and *Laser Interferometer Space Antenna - LISA*) decades in production. As telescopes and instruments get physically larger to collect and analyse more photons, the count rate for the number of components increases. Mass- and volume-budgets are fixed requirements and are applicable to both ground- and space-based astronomical hardware. For ground-based instruments,

*Further author information:

E-mail: carolyn.atkins@stfc.ac.uk

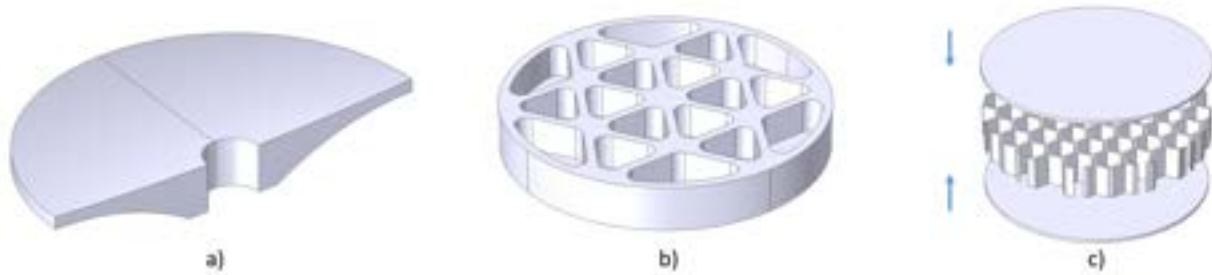


Figure 1. Lightweight mirror styles: *a)* contoured back, *b)* open-back, and *c)* sandwich

mass and volume-budgets are required to ensure that the instrument can enter the observatory and be located at the telescope focus, potentially requiring the use of heavy-duty lifting equipment. For space-based applications, the entire observatory is limited in mass and volume to ensure that it can be launched within the cargo payload of the rocket. Given the attributes of future astronomical hardware: bespoke, increasing component count, mass limits, and volume limits; new methods of component design and manufacture are required to build this future.

Additive manufacturing (AM; 3D printing) is a method of manufacture that creates an object, layer-by-layer, from a digital design file. AM exists in parallel with existing manufacturing methods, that is, AM does not replace an existing manufacturing method, rather it adds to the methods that already exist, for example, mill, drill and lathe (subtractive); casting and forging (formative); and fixing and bonding (fabricative). The primary advantage of AM is in the design freedom that can be gained, as the designer is no longer constrained by tool access. Intricate lattices and optimised structures can be integrated within a part design to reduce mass and part count with relative ease using AM. Given the design freedom, AM is ideal for bespoke and low yield component manufacture, where the objective of the design is to optimise for function, as opposed to a design to facilitate conventional manufacturing methods. As such, AM has the potential to offer a new paradigm in astronomical hardware design and manufacture.

One example of where the application of AM can support astronomical hardware is in the production of lightweight mirrors. Conventional lightweight mirrors fall within three categories: contoured back, open-back, and sandwich.¹ Contoured-back mirrors have a variable thickness to reduce mass (Figure 1 *a*), open-back mirrors remove mass from the underside of the mirror in pockets (Figure 1 *b*), and sandwich mirrors tend to be a composite of three components, two plates and an internal lightweight structure (Figure 1 *c*). In comparing lightweight mirrors, open-back and sandwich styles offer reduced mass in comparison to contoured mirrors. Open-back mirrors are easier to manufacture than sandwich mirrors; however, sandwich mirrors are more rigid.² Therefore, the question becomes, can AM be used to combine attributes from open-back (time & cost) with the attributes of sandwich mirrors (lower mass & more rigid).

Over the past decade a number of different organisations have explored metal lightweight AM mirrors using laser powder bed fusion (L-PBF)^{3–13} and electron beam powder bed fusion (EB-PBF).^{14,15} There are seven categories of AM and PBF represents the category where a layer of metallic powder is fused together using a heat source. The advantage of this method is that intricate structures can be achieved with relatively thin walls (~ 1 mm) providing a new design space for lightweight mirrors. In addition to metallic mirrors, AM ceramics have been investigated for mirror applications, such as alumina,¹⁵ silicon carbide variants^{16,17} and cordierite.¹⁵ Unlike the metal counterparts, AM ceramic mirrors have been created using a variety of AM categories, fused deposition modelling¹⁶ (FDM; filament), stereolithography¹⁵ (SLA; liquid resin) and binder jetting¹⁷ (powder + a binding agent). Beyond lightweight AM mirrors, there have been a number of investigations into AM for optical housings,^{18,19} opto-mechanical structures²⁰ and compliant mechanisms^{21–23} for astronomy or space-based applications.

However, there are several challenges associated with the uptake of AM within astronomical hardware. One of the key practical challenges is the lack of standardisation within AM, which results in a wide range in quality of the printed part. That is, the operation of identical machines can vary depending whether the primary use is as an external AM bureau, where successful prints are the priority, or in a research environment where a specific

AM material quality is required. For example, the number of times the metal powder is recycled in PBF affects the quality of the printed substrate. A further practical challenge is variability in material properties, where, for example, the Young's Modulus (E) of a material is likely to be different in the build direction (E_z) than in the in-plane directions (E_x, E_y). Finally, AM defects, such as porosity, fractures and inclusions, can result in substrates that are not fully dense and potentially have increased likelihood of failure by fracture or yield.

In addition, there are less tangible challenges to solve for the implementation of AM within astronomical hardware, such as Design for AM (DfAM) skills, upskilling engineers and machinists, and incorporation of AM within a very risk averse field. To successfully design for AM, where success is defined as a design that is optimised for function, printing and machining, requires a new set of design skills beyond the conventional computer aided design (CAD) packages. Freeform organic structures and lattices provide the engineer with a new design space to optimise for reduced mass, limited volume and specific loading conditions, and there are a number of software packages, or software extensions, which offer this capability. However, not all AM designs that have been optimised for function can be printed, due to specific design rules associated with a given printer, particularly in terms of orientation to the build platform and heat transfer for PBF processes. Further, how the AM part will be machined is fundamental to ensure that it can interface appropriately with the neighbouring components and a new challenge arises in how to machine a near-net shape. Ultimately, upskilling of design engineers and machinists is required to enable successful adoption of AM, but this is challenging given a demanding schedule of project delivery and counteracting potentially decades of experience in designing and machining for subtractive manufacture. Finally, astronomical projects, particularly for space-based or high-cost ground-based applications, are risk averse where component designs with existing heritage are preferred.

This paper summarises a research programme aiming to address some of the physical and intangible challenges which limit AM adoption within astronomical hardware. The focus of the programme is towards lightweight AM mirrors for space-based applications; however, a broader investigation into astronomical hardware in general is also considered. The programme draws upon two parallel research streams, the first considers the implementation of AM design in astronomical hardware and the second investigates the material properties of AM specifically for mirror fabrication. Supporting the research streams are two future looking work packages: space or environmental qualification, and training and engagement. Section 2 introduces the research programme in context; Section 3 presents the first case study investigating AM for an opto-mechanical application; Section 4 presents a second case study exploring AM for a lightweight deployable mirror petal; and Section 5 explores optimising the AM print parameters and post-processing steps. The paper closes with a discussion what the community will potentially lose by not adopting AM in Section 6 and a summary of the paper in Section 7. Data relating to the case studies can be accessed via Section 8.

2. AM4SPACE - A FOUR-YEAR RESEARCH PROGRAMME

The colloquially named AM4Space programme, has the primary goal to create a strategy for the adoption of lightweight AM mirrors within future space-based telescopes; however, more broadly the programme considers astronomical hardware, both ground- and space-based. AM4Space is funded through UK Research and Innovation (UKRI) via the Future Leaders Fellowship scheme. To enable the delivery of the strategy for adoption of AM mirrors there are four objectives:

1. to explore the AM design freedom and to develop design strategies for difference mirror geometries;
2. to optimise AM print parameters and post-processing to ensure high reflectivity at wavelengths of interest;
3. to undertake qualification of AM substrates for operational environments;
4. and, to engage a broad community to highlight potential AM and to increase user confidence.

The approach of AM4Space to deliver these objectives blends student-led case studies, with more conventional research and development. The AM design freedom is broken down into individual case studies, where an undergraduate student undertakes a one-year placement within the AM4Space team to explore the design freedom for a given application, examples from 2022/2023 include an optomechanical structure (Section 3) and a deployable

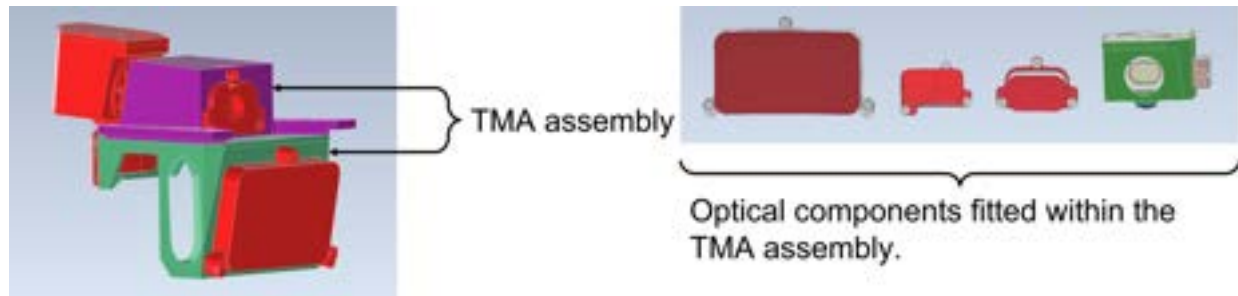


Figure 2. The METIS TMA assembly for AM redesign. Image credit: UKATC/METIS

mirror for Earth observation (Section 4). The student-led design case studies is a deliberate response to the need for future mechanical engineers leaving higher education to have a practical understanding in both subtractive and additive manufacturing methods. Print parameters, post-processing and qualification are researcher led in order to benefit from experience in the field.

3. OPTOMECHANICAL STRUCTURES

In this section, a summary of the case study presented in *Wells, J. T., et al. (2023)*²⁴ is provided. The CAD files generated from this study can be accessed via the link provided in Section 8.1.

3.1 Motivation

One beneficiary of using AM for astronomical hardware is the creation of lightweight, rigid geometries for opto-mechanical structures. Similar to the optical components that are mounted in them, opto-mechanical structures are frequently bespoke items, which are designed for a given instrument or telescope. The size of opto-mechanical structures varies significantly from centimetres to meters, which means that the potential mass saving could be in the 10s or 100s of kilograms.

3.2 Design brief

The goal of this case study was to explore the design freedom and challenges of using AM to create lightweight opto-mechanical structures for future instruments related to the next generation of 30 m class telescopes: the ELT, the Giant Magellan Telescope and the Thirty Meter Telescope. The specific case study focussed on a three mirror anastigmat (TMA) assembly within the mid-infrared ELT imager and spectrograph²⁵ (METIS) instrument. The objectives in using AM for this case were:

1. to use design optimisation tools to reduce the mass of the TMA assembly whilst meeting structural performance criteria;
2. to reduce the number of parts in the assembly;
3. to determine the suitable AM category and technology to enable production of the opto-mechanical redesign and evaluate relevant AM samples.

3.2.1 The METIS TMA assembly

Figure 2 presents the selected TMA assembly design for manufacture and the dimensions are approximately $0.6\text{ m} \times 0.5\text{ m} \times 0.5\text{ m}$. The assembly has two main structures, which are fixed together with 28 fasteners, and the assembly has a combined mass of 27.6 kg. The material of the assembly, excluding the fasteners, is aluminium 6061, and the operational environment is 70 K and 10^{-6} Pa. The European Southern Observatory (ESO) defined the acceptance criteria for the TMA assembly and in this study, a subset of three criteria within the operational environment were selected as a benchmark for success: maximum stress during a quasi-static earthquake equivalency; the modal eigenfrequency; and the wavefront error under gravitation loading.

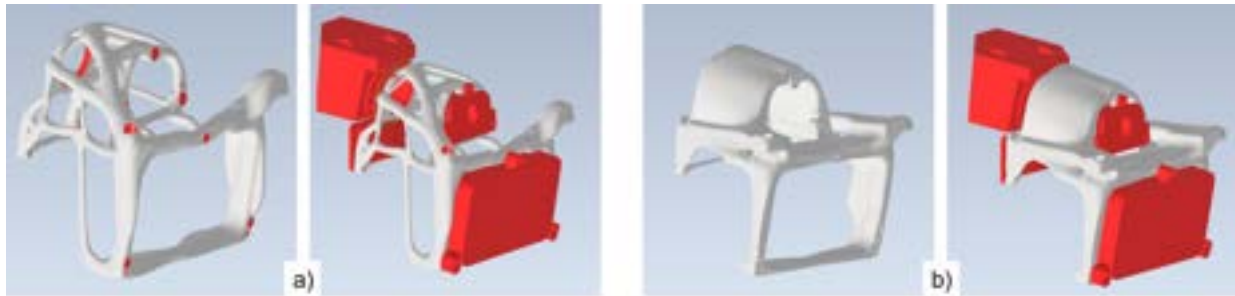


Figure 3. The AM redesign of the TMA assembly: *a)* the topology optimised design; and *b)* the varied wall thickness design.

3.3 Method

3.3.1 Design for AM - software

Three software tools were used to create two AM redesigns of the TMA assembly: commercial CAD, commercial finite element analysis (FEA), and a dedicated AM design package. The AM design package was used to create the optimised structure from a given loading condition; the AM design was passed to the CAD package to add the interfacing surfaces, for example the plane faces which locate with the mirror mounts; and FEA was used to ensure that the AM design met the ESO criteria.

3.3.2 Direct energy deposition - WAAM

The AM category direct energy deposition (DED) was identified as the current optimum method for printing large metallic structures. DED uses a metallic source material (powder or wire) which is aligned with a heat source (laser or electric arc), to locally deposit metal to create a freeform structure. The DED technology wire arc additive manufacturing (WAAM) uses metal wire and an electric arc mounted onto a robotic arm to print the structure. WAAM was selected due to its capability to create large structures and a variant of this technology has been successfully used to '3D print rockets'.²⁶

3.3.3 WAAM evaluation

To explore the WAAM technology, eight samples were printed in aluminium 5356, four samples had the geometry of a cuboid and four the geometry of a box. The geometries were defined to meet the preferred operational sample requirements of the in-house outgassing rig,²⁷ which was used to quantify the potential of the WAAM samples to outgas within a vacuum relative to a conventional subtractively machined sample. An internal evaluation of the samples to quantify printing defects was undertaken using X-ray computed tomography (XCT).

3.4 Results

Figure 3 presents two different approaches to design optimisation for the TMA assembly. Figure 3 *a)* highlights the use of topology optimisation, where a start volume, represented by a 3D mesh, is reduced in mesh elements based upon user defined criteria and a loading condition, for example, the quasi-static earthquake condition. Figure 3 *b)* presents a bespoke varied wall thickness optimisation, where an initial shell around the optical path was increased and decreased in thickness based upon the stress map resulting from a loading condition. Both designs met the target ESO criteria that were evaluated, consolidated 30 parts into one, and represented a mass reduction of 41% and 27% for the topology optimised and the varied wall thickness design respectively. Comparing the two designs to the geometry constraints of WAAM, the varied wall thickness design is preferred due to the continuous geometry when cross-sectioned - a continuous geometry is preferred as it prevents a stop-start of the electric arc.

Figure 4 presents the WAAM samples printed in Al 5356, both before and after machining from the build platform. The surface of the samples prior to machining indicated some small pinholes; however, millimetre-scale porosity was observed post machining (Figure 4 *a)* left). XCT analysis quantified the porosity within one sample of each geometry type using the Otsu thresholding method, a WAAM cuboid exhibited 2.67% porosity and a



Figure 4. The samples created using WAAM for evaluation: *a)* a WAAM block and machined box; and *b)* a WAAM box and machined rectangular tube.

WAAM box exhibited 3.83% porosity. A porous structure is non-desirable for a vacuum environment due to an increased likelihood of outgassing over time. Results from measuring the outgassing rates of three WAAM machined boxes and three WAAM machined tubes highlighted an approximate factor of 10 increase relative to conventionally machined bulk aluminium.

3.5 Discussion & future work

The optimised TMA assemblies presented in Figure 3 represent a first step in the design phase. Further design iterations need to be made in collaboration with WAAM operators and downstream machinists, to ensure that the TMA assembly is optimised for function, printing, and machining, to create an operational component. However, the optimised designs presented demonstrate the potential of AM to reduce mass and part count, whilst meeting operational criteria.

The porosity observed in the WAAM samples is detrimental for a cryogenic vacuum environment and fatigue life. The presented samples represent the first trial of the supplier to use WAAM with aluminium and through discussion it is likely that the observed macro-porosity originated with a gas flow that was too high which created turbulence within the melt pool. Therefore, by optimising the WAAM parameters specifically for aluminium, a less porous print can be achieved, providing confidence in the use of WAAM to create opto-mechanical structures for astronomy in the future.

4. AM MIRROR DEVELOPMENT

In this section, a summary of the case study presented in *Westsik, M., et al. (2023)*,²⁸ which was presented at this conference, is provided. The CAD files generated from this study can be accessed via the link provided in Section 8.2.

4.1 Motivation

The primary benefits of lightweight (low-mass) AM mirrors for astronomy, introduced in Section 1, link combining the attributes of open-back mirror (time & cost), with those of sandwich mirrors (lower mass & more rigid). A further benefit is the reduction of parts, which in the case of AM mirrors can include the mounting structure used to interface the mirror with the optical payload.

4.2 Design brief

The goal of this study was to investigate the AM design freedom for lightweight mirror fabrication, whilst considering and implementing the different stages of manufacture: metal printing, subtractive machining, and single point diamond turning (SPDT). The case study selected was one of the deployable M1 petals of the 6 U nano-satellite ISAAC²⁹ (Integrated Space Active Optics for Aberration Compensation). The objectives for using AM in this study are:

1. To reduce the mass of the AM design by $\sim 50\%$ using lattice structures, to prioritise rigidity by using a lightweight sandwich mirror structure and to reduce the part count.



Figure 5. The deployed ISAAC optical assembly (*left*) and the non-reflective underside of the M1 petal for redesign (*right*). Image credit: UKATC/ISAAC

2. To integrate design for AM, design for manufacture and design for optical manufacture practices within the final design.
3. To design, print, manufacture and evaluate the prototype(s), to highlight how the final design can be created.

Note - there are no objectives relating to the optical quality; the focus is design and manufacture.

4.2.1 The ISAAC M1 deployable mirror petal

The ISAAC deployable M1 assembly and the mirror petal identified for AM design, are highlighted in Figure 5 *left*. The mirror petal has nominal dimensions 192 mm × 106 mm × 42 mm, a parabolic concave optical prescription, and will be subtractively machined from aluminium. The reverse of the mirror petal, shown in Figure 5 *right*, includes further components that are used to interface the petal to the M1 assembly. The petal including the interfacing components have a total part count of 9 and a mass of 437 g. The AM redesign retains the nominal dimensions and interfaces from the ISAAC design; however, the optical prescription is simplified to spherical concave, with a radius of curvature of 628 mm.

4.3 Method

4.3.1 Lattice downselection

Dedicated AM design software packages enable the rapid generation of a variety of lattice structures. The specific software used in the case study had 33 lattices available to the user and therefore an assessment of the suitability of each lattice to act as a mirror lightweight structure was undertaken. In a first iteration of the downselection, lattices were excluded on the principle of ‘printability’, that is, how suitable is the lattice as an internal lightweight structure given the constraints of L-PBF. A second and third iteration used FEA to evaluate the performance of the lattice given different loading conditions; Figure 6 *left* presents the average surface displacement as a function of weight remaining for a perpendicular load, the optimum lattices in the graph are those identified with low displacement and low weight remaining. In a final iteration of downselection, polymer prototypes were created of the four remaining lattices to assess the ability of the lattice to allow metal powder removal. In this practical iteration, the transparent prototypes were filled with red sand, to simulate the metal powder, and the ease at which the sand could be removed was assessed using video recordings - a video frame is shown in Figure 6 *right*.

4.3.2 Manufacture

Three distinct manufacturing steps were required to convert the AM design into a physical aluminium prototype: additive manufacturing, subtractive manufacturing, and optical manufacturing. L-PBF was identified as the first choice technology for printing the AM design, the selection was based upon a suitable print resolution to accurately recreate the lattice structures; the material choices available and the requirement for no binder material; and previous local experience using L-PBF for mirror manufacture. An external AM bureau was identified that operated a printer with a large build volume (500 mm × 280 mm × 320 mm) in aluminium (AlSi10Mg), which could accommodate the prototypes.

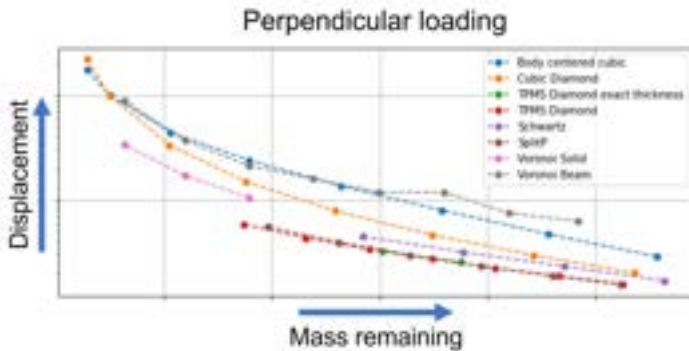


Figure 6. Lattice downselection: *left* displacement as a function of mass for perpendicular loading of a sandwich lattice structure; *right* the sand test used for the final downselection.

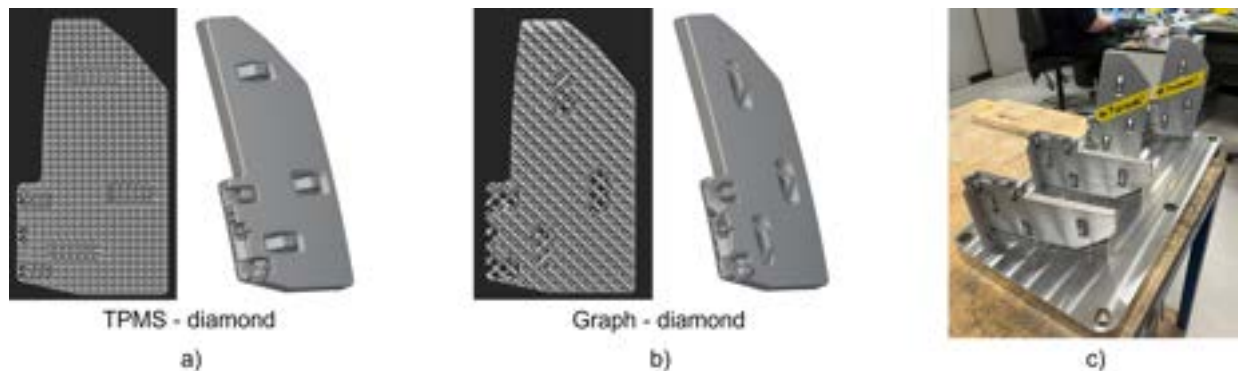


Figure 7. The final prototype designs: *a*) the selected TPMS Diamond lattice; *b*) the selected Graph Diamond lattice; and *c*) the as-printed design upon the build platform, image credit: G. Campbell.

Subtractive manufacturing (milling and turning) and optical manufacturing (single point diamond turning; SPDT) were used to convert the AM aluminium print into a functional mirror. Close collaboration was needed between the machinists and the designer to ensure that the output near-net shape aluminium print could be machined with the required interfacing surfaces. To facilitate ease of machining, sacrificial features were incorporated within the AM design.

4.3.3 Metrology

To evaluate the AM mirror prototype, internal and external dimensional metrology was undertaken. The as-printed AM substrates were evaluated using external contact profilometry to determine the radius of curvature of the would-be mirror surface and XCT measurements (voxel size = $60\ \mu\text{m}$) to quantify the internal porosity and fidelity of the print compared with the print file. The optical surfaces of the SPDT prototypes were evaluated for micro-roughness using a Bruker Contour GT-X stitching microinterferometer at three magnifications: $\times 2.5$, $\times 10$, and $\times 50$.

4.4 Results

Following the FEA and sand test downselection two lattices were selected for prototyping: TPMS Diamond and the Graph Diamond. The difference lattice geometries required a different build orientation for each lattice which impacted the DfAM of the mounting features. The internal lattices and final designs for printing are highlighted in Figure 7 *a*) and *b*). The final designs achieved a $\sim 44\%$ mass reduction and consolidation of nine parts into one.

Two prototypes of each design were successfully printed at the external AM bureau, as shown in Figure 7 *c*). The external support material visible in Figure 7 *c*), was required to allow heat dissipation during build and was removed by the bureau prior to delivery. On receipt of the prototypes, one set (one TPMS & one

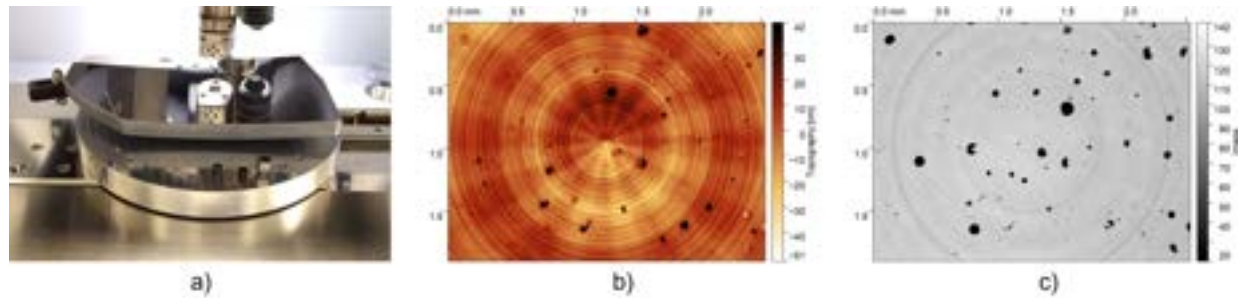


Figure 8. Micro-roughness measurements on the SPDT Graph prototype: *a)* the prototype under measurement, image credit I. T. Nistea; *b)* the topography map at ROI 3, the centre of SPDT; and *c)* the microscope image to accompany ROI 3 topography map.

Graph) was sent for XCT measurements and the second set was sent for machining and SPDT. The TPMS prototype was machined first; however, due to the challenges of machining near-net shapes, an error occurred which resulted in more material removal than required which impacted the optical surface. The machining of the Graph prototype, which built upon the previous experience, led to a successful completion of the manufacturing process chain resulting in an optical surface for evaluation.

A first analysis of the $60\ \mu\text{m}$ voxel XCT data focussed on porosity, extracting information relating to the size and location of the pores relative to the optical surface. The results indicated that the majority of the porosity was located within $0.5\ \text{mm}$ measured normal from the optical surface and that the porosity was located towards the centre of the prototype. However, the voxel grey-scale contrast of the XCT data varied in the region of interest (the $2\ \text{mm}$ thick optical surface), which results in low confidence that the segmentation of the pores, from the aluminium, accurately represents the porosity. In addition, the voxel size limits the porosity that can be measured, the resolution limit for features within XCT data is typically stated at $\sim 2 \times \text{voxel size}$, which restricts the pore size that can be measured to $\sim 120\ \mu\text{m}$ in the described data. However, it should be noted that a single voxel, or a pair of voxels, would also be difficult to distinguish from measurement noise and therefore, result in a low measurement confidence.

The presence of porosity, observed in the XCT analysis, was confirmed in the micro-roughness measurements, as shown in Figure 8. Five regions of interest (ROI) located towards the centre of the spherical curvature, where the surface was less tilted, were measured. The root mean square (RMS) micro-roughness values for $\times 2.5$ magnification ranged from $314\ \text{nm}$ to $4.2\ \text{nm}$. The ROIs which exhibited high roughness values were subject to both SPDT ‘pick-up’ scratches and porosity; however, the low roughness value of $4.2\ \text{nm}$ RMS, does highlight the potential of the AM aluminium substrate to deliver $\lesssim 5\%$ scatter in the visible and infrared wavelengths, estimated assuming a Gaussian roughness profile and light at normal incidence.

The porosity observed in the microscope images (Figure 8 *c)*) was used to estimate the porosity $< 60\ \mu\text{m}$ in size by exploiting the $\sim 4\ \mu\text{m}$ pixel size of the microscope images. Using the same XCT analysis method, it was found that, on average, only $\sim 16\%$ of pores within the microscope image field of view are $> 60\ \mu\text{m}$, thereby necessitating an alternative approach to acquiring XCT data to reduce voxel size in the future.

4.5 Discussion & future work

The study was successful in achieving the goal to investigate the AM design freedom for lightweight mirror fabrication, whilst considering and implementing the different stages of manufacture. The AM design freedom was explored to select the optimum lattices for function, as well as to consolidate nine components into one. The final designs incorporated DfAM geometry features, mounts for subtractive machining, as well as mounts to connect the prototype to the optical assembly. Four aluminium prototypes have been printed and one prototype has been successfully taken through all the manufacturing steps to date. However, lightweight mirrors for astronomy and Earth observation are bespoke and therefore it cannot be assumed that the designs created in this study can be directly translated into another project. To create a design strategy for lightweight AM mirrors, different mirror geometries and optical prescriptions need to be considered and a suitable approach for AM design identified. This case study represents a first chapter in a broader strategy.

Future work will focus on exploring different optical geometries and prescriptions to deliver the broader strategy, with case studies now underway investigating a cylindrical convex geometry with attachments to a deployable boom; and an approximately square concave geometry with the goal to remove $\sim 70\%$ of the mass in comparison to the conventional design. It is hoped that future case studies will explore hexagonal and freeform geometries.

5. AM MATERIAL INVESTIGATION

This section draws upon content introduced by *Snell, R. M. et al. (2022)*³⁰ and presents new dimensional metrology data.

5.1 Motivation

The benefits of the AM design space have been introduced and applied to create structures optimised for their function. However, as presented in Sections 3 and 4, AM material properties remain a barrier in the adoption of AM within astronomical hardware. At the outset of the AM4Space programme, the AM materials research stream was decoupled from design stream to allow the streams to run in parallel, with the programme uniting the streams in the final year. The goal of this research stream is to identify print parameters and post-processing steps that provide an optimal substrate for AM mirror production.

5.2 Method

5.2.1 AM print parameters

AM print parameters, in the context of this paper, refer to the L-PBF printer settings, aluminium powder, and the part set-up within the print environment. The focus on the L-PBF technology stems from its frequent use in metal AM mirror production. Each L-PBF printer has numerous parameters that can be adjusted to enable a print, for example, a non-exclusive list includes:

1. Layer height - the thickness of one printed layer, typically $\sim 30\ \mu\text{m}$ to $100\ \mu\text{m}$;
2. Temperature - the thermal environment of the print;
3. Powder history - how often the powder has been recycled;
4. Laser power - the energy applied to melt the powder;
5. Laser speed - how quickly the laser creates the solid part cross-section within the powder;
6. Print path - the route the laser takes across the powder.

How the part is orientated within the print environment also affects the resultant AM material quality, as the orientation links to the print path, which in turn links to the temperature.³⁰ The temperature in turn links to the likelihood of porosity, where lack of fusion pores result when the print environment is too cold and keyhole pores result when print environment is too hot - it is suspected that the pores visible in Figure 8 *b)* and *c)* are keyhole pores.

In the presented study, the objective was to determine the effect of build orientation and a heat treatment applied in post-processing, to the surface roughness after SPDT. The sample geometry for the study is shown in Figure 9 *a)*, the diameter and height are 50 mm and 5 mm respectively, there is a 1 mm chamfer applied to the flat optical surface and three lugs are added to the design to aid mounting and handling. Three build orientations were evaluated: 0° (in the plane of the build platform), 45° , and 90° . Two sets of samples were created, each set containing one 0° , one 45° and two 90° ; Figure 9 *b)* highlights the build platform with the 45° and 90° samples after printing.

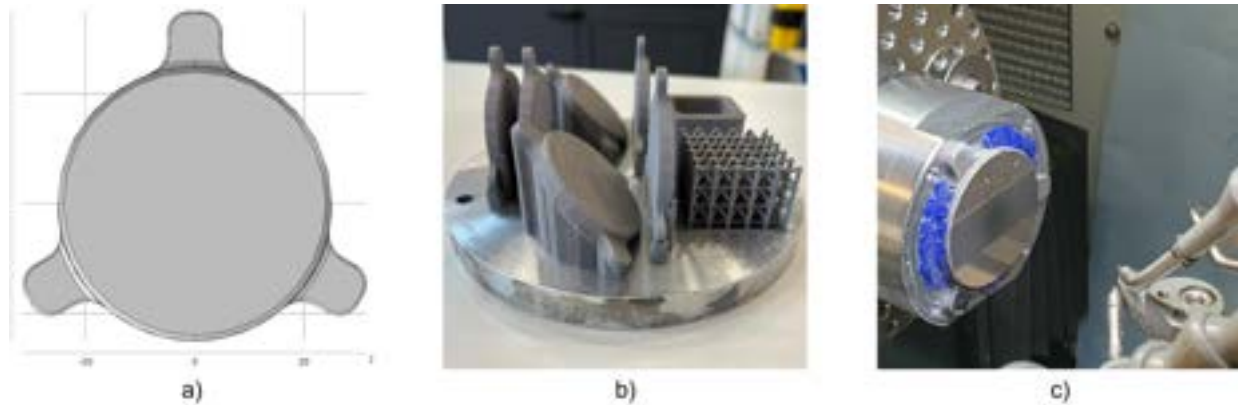


Figure 9. Sample production: *a)* the sample design, 50 mm diameter 5 mm height; the aluminium samples on the the build platform, image credit: R. M. Snell; and *c)* the SPDT of a sample, image credit: M. Harris.

5.2.2 Post processing

There were three steps in the post-processing: removal of the support material, seen in Figure 9 *b)*, through subtractive machining; a heat treatment applied to one set of samples; and SPDT to generate a reflective surface. A hot isostatic press (HIP) was used to deliver the heat treatment, this method places the samples within a pressure vessel and applies high pressure and high temperature. HIP has been successfully used to close porosity and to reduce the anisotropic material behaviour in AM aluminium parts;³¹ however, it should also be noted that pore regrowth has been seen in HIP-ed AM titanium following further thermal annealing.³² Following HIP treatment, the two sets (one HIP and non-HIP) were SPDT, as shown in Figure 9 *c)*.

5.2.3 Evaluation

The samples after post-processing were visually inspected (by-eye and microscope) and a qualitative assessment of the reflective surface was noted. A quantitative analysis of the reflective surfaces was undertaken using a Bruker Contour GT-X stitching micrometer at three magnifications: $\times 2.5$, $\times 10$, and $\times 50$. Three regions were measured on each sample: the centre of SPDT (0, 0), a 12.5 mm y-displacement (0, 12.5), and a 12.5 mm x-displacement (12.5, 0).

5.3 Results

The reflective SPDT samples from both the HIP and non-HIP are shown in Figure 10. A complete qualitative assessment is provided in *Snell, R. M. et al., (2022)*;³⁰ however, in summary, the non-HIP samples exhibited irregular porosity and SPDT scratches in all three orientations, and the HIP samples exhibited low \rightarrow zero porosity or scratches, but the reflectivity was less and the samples appeared ‘milky’, implying increased scatter.

Evaluating the sample quantitatively using the micrometer confirmed the qualitative visual inspection. Table 1 presents the roughness parameters for the average of the three measurement regions for the eight samples. The average roughness (S_a) and RMS roughness (S_q) confirm that the roughness is higher for the HIP samples than the non-HIP; however, the peak-to-valley (S_z) is lower for the HIP samples, implying the reduction of localised defects on the surface in comparison to the non-HIP. The topography images, comparing print orientations and post-processing, are presented in Figures 11 to 13. Porosity and SPDT scratches are evident in the non-HIP topography images, in addition, the L-PBF melt pools are also visible. In contrast, the HIP topography maps highlight a non-stochastic ‘noisy’ surface, where the noise is orientated with the SPDT cutting lines.

In Table 1, 90° non-HIP #2 and 90° HIP #2 present higher roughness values than 90° non-HIP #1 and 90° HIP #1. For 90° non-HIP #2 the increased roughness is due to the central (0, 0) region exhibiting more surface defects (porosity) and hence increased roughness than the neighbouring datasets, thereby biasing the average. For 90° HIP #2, each measured region exhibited approximately the same roughness value (S_q range: 22.8 nm to 26.0 nm), implying a difference in either the AM substrate or the effect of the post-processing. Given the limited and variability of the dataset, a link between print orientation and roughness cannot be confirmed. Further,

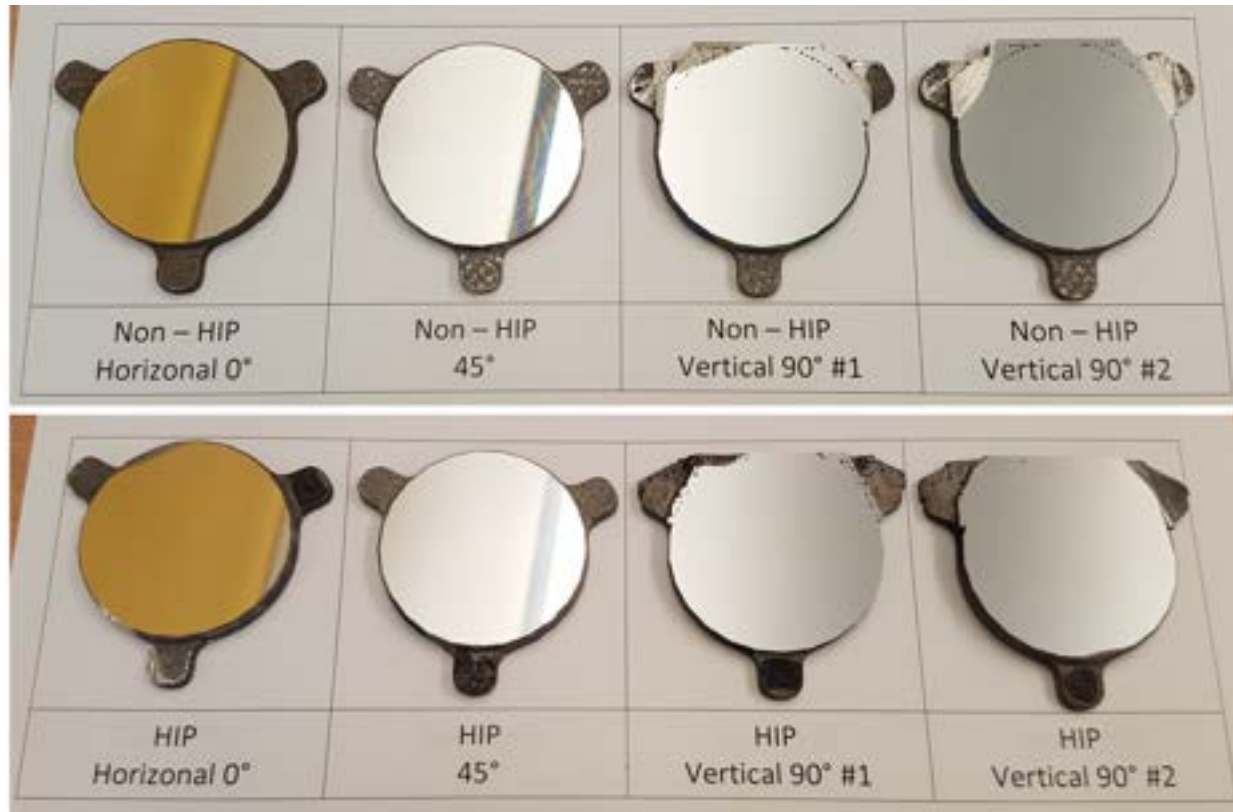


Figure 10. All eight SPDT samples: non-HIP (*top*) and HIP (*bottom*).

Table 1. The surface roughness parameters averaged over the three measurement regions for each sample.

Sample	Sa [nm]	Sq [nm]	Sz [nm]	Sample	Sa [nm]	Sq [nm]	Sz [nm]
90° - non-HIP # 1	6.3	8.5	440	90° - HIP # 1	10.7	11.8	260
90° - non-HIP # 2	10.8	16.5	657	90° - HIP # 2	18.9	24.1	470
45° - non-HIP	5.7	9.0	460	45° - HIP	9.9	12.8	340
0° - non-HIP	7.1	11.1	430	0° - HIP	9.5	12.6	303

Sa - average, Sq - RMS, Sz - peak-to-valley

questions remain whether this first trial of HIP and SPDT is representative, as the feedback from the thermal sensors within the HIP suggest that a HIP temperature much higher than standard was applied. An error during the HIP meant that the target temperature (500 °C) was exceeded and a constant temperature of ~570 °C was recorded over the 4 hrs of the HIP heating phase. This temperature is higher than commonly used for L-PBF aluminium³¹ (510 °C to 540 °C) and, as such, the effect the aluminium micro-structure is unclear. Therefore, the role of HIP on surface roughness after SPDT requires further investigation.

5.4 Discussion & future work

One of the barriers faced in the adoption of AM prints for mirrors substrates is ensuring a defect free material. Work is on-going to determine the optimum print parameters and post-processing routes for aluminium intended for mirror applications. The preference to optimise the print parameters, rather than coat the AM substrate in nickel phosphorus¹⁴ (NiP), which is commonly used in metal mirror manufacture, stems from a desire to reduce the processing steps and to remove the mismatch in coefficient of thermal expansion between the aluminium and the NiP.

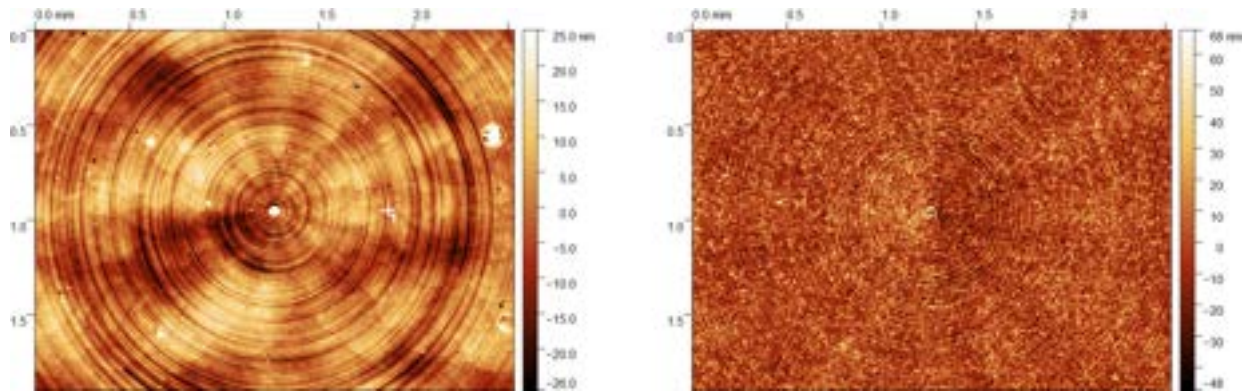


Figure 11. $\times 2.5$ magnification: (left) 90° non-HIP #1 (0, 0); and (right) 90° HIP #1 (0, 0).

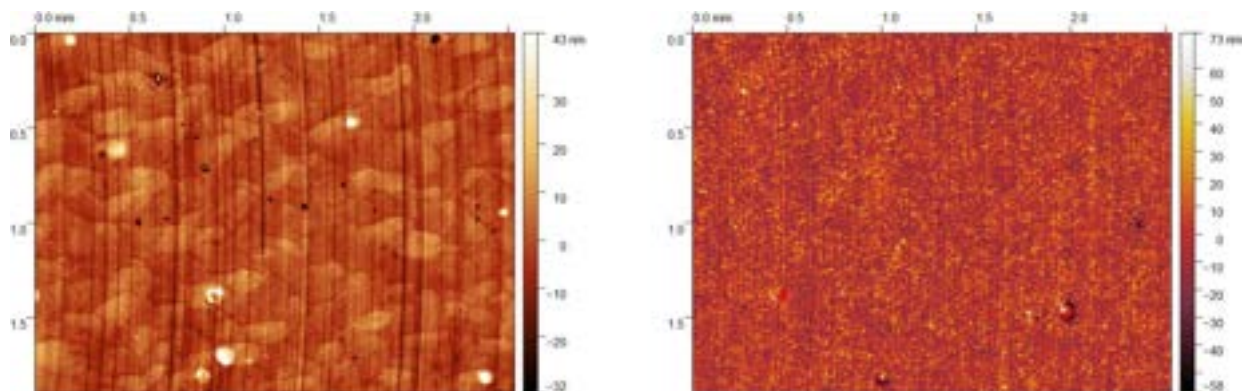


Figure 12. $\times 2.5$ magnification: (left) 45° non-HIP (12.5, 0); and (right) 45° HIP (12.5, 0).

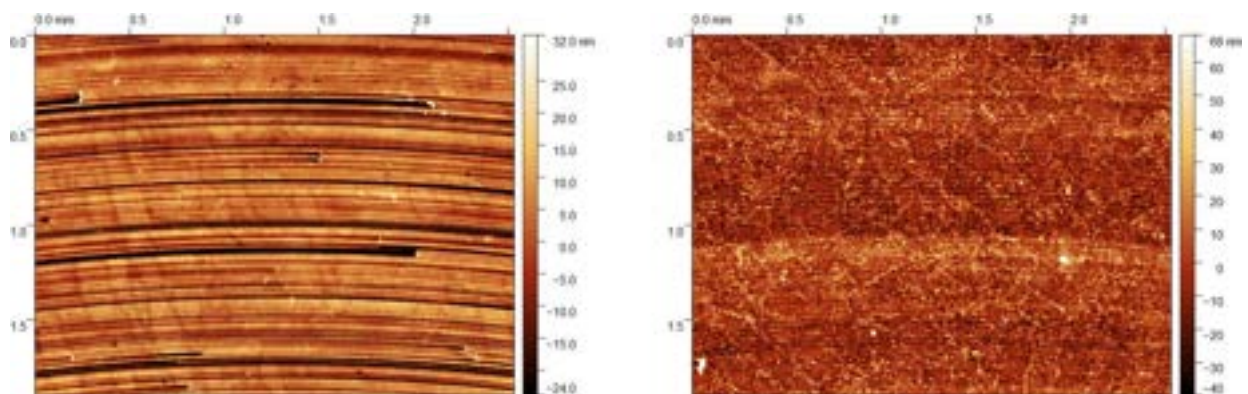


Figure 13. $\times 2.5$ magnification: (left) 0° non-HIP (0, 12.5); and (right) 0° HIP (0, 12.5).

On-going and future work is divided into parallel efforts: first, a repeat of the study presented in this paper with the appropriate HIP temperature; and second, an investigation into the material micro-structure. The repeat of the presented study explores the effect of HIP, both internally using XCT and externally through SPDT and surface roughness measurements. The objective is that the effect of HIP on porosity can be quantified using XCT before and after treatment. In addition, different HIP providers will be used to assess the different HIP parameters. The second effort to evaluate the presented samples micro-structure, aims to investigate the difference in material structure between the HIP and non-HIP aluminium. It is hoped that these measurements could help inform suitable print parameters and post-processing routes in the future.

6. DISCUSSION

The astronomical instrumentation community has incredible ambitions for ground- and space-based observatories in the future; however, as a community it is also risk averse and relies frequently on existing design heritage, which may be 10, 20, 30+ years old. Minimising risk, particularly within large, international projects, is prudent given the tax-payer is frequently the funding source, but what do we lose by not considering new routes of manufacture? AM is a method of manufacture which will soon be considered on-a-par with subtractive, formative and fabricative methods, and already it has been adopted in alternative fields, such as healthcare³³ and aerospace.³⁴ Therefore, the time is right to start considering the use of AM at the outset of new astronomical instrumentation projects.

Parallels can be drawn with the construction industry, which, similar to international observatory projects, deliver unique, one-of-a-kind constructions and frequently involve numerous stakeholders and partners. A paper by *Olsson, N. O. E., et al. (2021)*³⁵ describes the barriers and enablers of integrating concrete 3D printing within the construction industry. There are many similar barriers preventing the adoption of AM in construction projects, for example, “risk in adopting new technology” and “high cost of the innovation”.³⁵ However, enablers from construction also apply: “An important issue for architecture as a field will therefore be whether or not architects are ready to make use of the complex, potential and the high degree of design freedom provided by additive construction. . .”,³⁵ and “Ideally, the design process should be thought of as a collaboration between architects, engineers and constructors.”³⁵ In this context, architect could be considered as the Principal Investigator or Head Engineer, but the parallels remain, particularly in the collaboration of individuals with a stake in the design: systems engineers, mechanical engineers, AM design engineers, AM operators, machinists, and assembly, integration & test (AI&T) specialists. Following the Astro2020 decadal,³⁶ imminent planning and technology maturation for the top priority large space-based initiative, newly termed *Habitable Worlds Observatory (HWO)*, is underway. Large space-based initiatives (*flagships*) are decades in production and therefore, now is ideal opportunity to adopt AM at the outset of the proposal, when technology maturation is commencing.

7. SUMMARY AND CONCLUSION

This paper has introduced the benefits and challenges of using AM in astronomical hardware through a description of a four-year research programme, which has the goal to create a strategy for the adoption of lightweight AM mirrors within future space-based telescopes, and more broadly, AM adoption in astronomical instrumentation. Two AM design case studies were summarised: an opto-mechanical structure for METIS, a future instrument for the ELT; and, a lightweight mirror petal, forming part of an optical assembly within a 6U CubeSat. Both AM design case studies considered how the AM design could be created, and the accompanying prototypes and samples highlighted the challenges often encountered using AM, namely, material defects. To meet this challenge, research was presented highlighting the initial phase of the optimisation of AM print parameters and post-processing routes.

Adopting a new method of design and manufacture does require new skills, both technical and professional. AM, which is part of a larger industrial revolution - Industry 4.0³⁵ - will increasingly become mainstream within manufacture and therefore, it is inevitable that increasingly components will be made in this method. To ensure the benefit of AM is harnessed within the astronomical instrumentation community, engineers, technical specialists and managers need to be trained in the different aspects of AM and how its potential can be harnessed. To conclude, AM does not replace subtractive, formative or fabricative manufacture methods, rather it has the potential offer new design solutions whilst working in parallel with the existing methods.

8. DATA AVAILABILITY STATEMENT

8.1 Optomechanical structures

The CAD files for both the topology-optimised design and varied wall thickness design are openly available from eData, the STFC Research Data repository, at <https://edata.stfc.ac.uk/handle/edata/938>.

8.2 AM mirror development

The as-printed and post-processed STL files presented in this paper are openly available from eData, the STFC Research Data repository, at <https://edata.stfc.ac.uk/handle/edata/937>.

ACKNOWLEDGMENTS

The authors acknowledge the UKRI Future Leaders Fellowship ‘Printing the future of space telescopes’ under grant # MR/T042230/1.

The authors acknowledge the Henry Royce Institute for Advanced Materials for access the Aconity3D Aconity-LAB facilities at The Royce Discovery Centre at the University of Sheffield, funded through EPSRC grants EP/R00661X/1, EP/S019367/1, EP/P02470X/1 and EP/P025285/1.

R. Snell & I. Todd acknowledge the EPSRC Future Manufacturing Hub in Manufacture using Advanced Powder Processes (MAPP) EP/P006566/1.

REFERENCES

- [1] Vukobratovich, D., [*Optomechanical Engineering Handbook - Chapter 5: Lightweight Mirror Design*], CRC Press LLC (1999).
- [2] Schwertz, K. and Burge, J. H., [*Field Guide to Optomechanical Design and Analysis*], CRC Press LLC (2012).
- [3] Herzog, H., Segal, J., Smith, J., Bates, R., Calis, J., De La Torre, A., Kim, D. W., Mici, J., Mireles, J., Stubbs, D. M., and Wicker, R., “Optical fabrication of lightweighted 3d printed mirrors,” *Proc. SPIE* **9573**, 957308–957308–15 (2015).
- [4] Sweeney, M., Acreman, M., Vettese, T., Myatt, R., and Thompson, M., “Application and testing of additive manufacturing for mirrors and precision structures,” *Proc. SPIE* **9574**, 957406–957406–13 (2015).
- [5] Woodard, K. S. and Myrick, B. H., “Progress on high-performance rapid prototype aluminum mirrors,” in [*Advanced Optics for Defense Applications: UV through LWIR II*], Vizgaitis, J. N., Andresen, B. F., Marasco, P. L., Sanghera, J. S., and Snyder, M. P., eds., **10181**, 177 – 182, International Society for Optics and Photonics, SPIE (2017).
- [6] Heidler, N., Hilpert, E., Hartung, J., von Lukowicz, H., Damm, C., Peschel, T., and Risse, S., “Additive manufacturing of metal mirrors for TMA telescope,” in [*Optical Fabrication, Testing, and Metrology VI*], Schröder, S. and Geyl, R., eds., **10692**, 92 – 98, International Society for Optics and Photonics, SPIE (2018).
- [7] Atkins, C., Feldman, C., Brooks, D., Watson, S., Cochrane, W., Roulet, M., Hugot, E., Beardsley, B., Harris, M., Spindloe, C., Alcock, S. G., Nistea, I.-T., Morawe, C., and Perrin, F., “Topological design of lightweight additively manufactured mirrors for space,” *Proc. of SPIE* **10706** (2018).
- [8] Hilpert, E., Hartung, J., von Lukowicz, H., Herfurth, T., and Heidler, N., “Design, additive manufacturing, processing, and characterization of metal mirror made of aluminum silicon alloy for space applications,” *Optical Engineering* **58**(9) (2019).
- [9] Tan, S., Ding, Y., Xu, Y., and Shi, L., “Design and fabrication of additively manufactured aluminum mirrors,” *Optical Engineering* **59**(1), 1 – 17 (2020).
- [10] Yan, L., Zhang, X., Fu, Q., Wang, L., Shi, G., Tan, S., Zhang, K., and Liu, M., “Assembly-level topology optimization and additive manufacturing of aluminum alloy primary mirrors,” *Opt. Express* **30**, 6258–6273 (Feb 2022).
- [11] Tan, S., Li, Q., Xu, Y., Shen, H., Cheng, Y., Jia, P., and Xu, Y., “Design and fabrication of lightweight additively manufactured mirrors for aviation,” *Appl. Opt.* **61**, 2198–2206 (Mar 2022).

- [12] Paenoi, J., Bourgenot, C., Atkins, C., Snell, R., Todd, I., White, P., Parkin, K., Ryder, D., Kotlewski, R., McPhee, S., Chanchaiworawit, K., Chartsiriwattana, P., Laoyang, A., Kuha, T., Leckngam, A., Buisset, C., Rujopakarn, W., and Poshyachinda, S., “Lightweight, aluminum, mirror design optimization for conventional and additive manufacturing processes,” in [*Advances in Optical and Mechanical Technologies for Telescopes and Instrumentation V*], **12188**, 121880U, International Society for Optics and Photonics, SPIE (2022).
- [13] Boschetto, A., Bottini, L., and Macrea, L., “Design and fabrication by selective laser melting of a lidar reflective unit using metal matrix composite material,” *The International Journal of Advanced Manufacturing Technology* **126**, 857–872 (May 2023).
- [14] Atkins, C., Brzozowski, W., Dobson, N., Milanova, M., Todd, S., Pearson, D., Brooks, D., Bourgenot, C., Snell, R. M., Sun, W., Cooper, P., Alcock, S. G., and Nistea, I.-T., “Additively manufactured mirrors for cubesats,” *Proc. of SPIE* **11116-41** (2019).
- [15] Roulet, M., Atkins, C., Hugot, E., Snell, R., van de Vorst, B., Morris, K., Marcos, M., Todd, I., Miller, C., Dufils, J., Farkas, S., Mezo, G., Tenegi, F., Vega-Moreno, A., and Schnelzer, H., “Use of 3D printing in astronomical mirror fabrication,” in [*3D Printed Optics and Additive Photonic Manufacturing II*], **11349**, International Society for Optics and Photonics, SPIE (2020).
- [16] Goodman, W. A., Nejhad, M. N. G., Minei, B. M., Stuecker, J. N., and Anderson, T. M., “Ultra-lightweight ultra-stable RoboSiC additively manufactured lasercom telescope,” in [*Material Technologies and Applications to Optics, Structures, Components, and Sub-Systems IV*], **11101**, 111010F, International Society for Optics and Photonics, SPIE (2019).
- [17] Horvath, N., Honeycutt, A., and Davies, M. A., “Grinding of additively manufactured silicon carbide surfaces for optical applications,” *CIRP Annals* **69**(1), 509–512 (2020).
- [18] Steele, I. A., Jermak, H., Bates, S., and Baker, I., “3D-printed optical instrumentation: practical starter designs and initial experiences,” in [*Advances in Optical and Mechanical Technologies for Telescopes and Instrumentation III*], **10706**, 107060S, International Society for Optics and Photonics, SPIE (2018).
- [19] Frasch, J., Hilpert, E., Hartung, J., Damm, C., and Heidler, N., “Optical housing made by additive manufacturing,” in [*Advances in Optical and Mechanical Technologies for Telescopes and Instrumentation V*], Navarro, R. and Geyl, R., eds., **12188**, 121880Y, International Society for Optics and Photonics, SPIE (2022).
- [20] Goodman, B., “The results of Goodman Technologies NASA Phase II SBIRs for additive manufacturing of mirrors and telescopes,” in [*Optical Manufacturing and Testing XIII*], Kim, D. W. and Rascher, R., eds., **11487**, 1148705, International Society for Optics and Photonics, SPIE (2020).
- [21] Saudan, H., Kiener, L., Perruchoud, G., Kruis, J., Vaideeswaran, K., Dadras, M. M., Cochet, F., and Liberatoscioli, S., “Compliant mechanisms and space grade product redesign based on additive manufacturing,” in [*Advances in Optical and Mechanical Technologies for Telescopes and Instrumentation III*], Navarro, R. and Geyl, R., eds., **10706**, 107062T, International Society for Optics and Photonics, SPIE (2018).
- [22] Kiener, L., Saudan, H., Cosandier, F., Perruchoud, G., Pejchal, V., Rouvinet, J., Boudoire, F., and Kalentics, N., “Validation of compliant mechanisms made by metallic additive manufacturing,” in [*Advances in Optical and Mechanical Technologies for Telescopes and Instrumentation V*], Navarro, R. and Geyl, R., eds., **12188**, 121880X, International Society for Optics and Photonics, SPIE (2022).
- [23] Morris, K., Atkins, C., Reynolds, L., Walpole, J., van de Vorst, L. T. G. B., Snell, R., Miller, C., Farkas, S., Mező, G., Roulet, M., Hugot, E., Vega-Moreno, A., Sanginés, F. T., and Schnelzer, H., “Additively manufactured flexure for astronomy instrumentation,” **12188**, International Society for Optics and Photonics, SPIE (2022).
- [24] Wells, J. T., Westsik, M., Chahid, Y., Macleod, A., Bissell, L., Kotlewski, R., McPhee, S., Orr, J., e Silva, M. P. E., McKegney, S., Cochrane, W., Breen, C., and Atkins, C., “Lightweighting large optomechanical structures in astronomy instrumentation utilising generative design and additive manufacturing,” **12669-21**, International Society for Optics and Photonics, SPIE (2023).
- [25] Brandl, B. R., Bettonvil, F., van Boekel, R., Glauser, A., Quanz, S. P., Absil, O., Feldt, M., Garcia, P. J. V., Glasse, A., Guedel, M., Labadie, L., Meyer, M., Pantin, E., Wang, S.-Y., van Winckel, H., Agócs, T., Amorim, A., Bertram, T., Burtscher, L., Delacroix, C., Laun, W., Lesman, D., Raskin, G., Salo, C., Scheithauer, S., Stuik, R., Todd, S., Haupt, C., and Siebenmorgen, R., “Status update on the development

of METIS, the mid-infrared ELT imager and spectrograph,” in [*Ground-based and Airborne Instrumentation for Astronomy IX*], **12184**, 1218421, International Society for Optics and Photonics, SPIE (2022).

- [26] Relativity Space, “Press release: RELATIVITY SPACE MAPS PATH TO TERRAN R PRODUCTION AT SCALE WITH UNVEIL OF STARGATE 4TH GENERATION METAL 3D PRINTERS.” <https://www.relativityspace.com/press-release/2022/10/24/relativity-space-maps-path-to-terran-r-production-at-scale-with-unveil-of-stargate-4th-generation-metal-3d-printers>. Accessed: 2023-09-10.
- [27] Breen, C., Walpole, J., Atkins, C., McPhee, S., Cliffe, M., Moffat, J., Edwards-Mowforth, M., Lister, I., Reynolds, L., Conley, A., Allum, S., Snell, R. M., Tammias-Williams, S., and Watson, S., “Outgassing properties of additively manufactured aluminium,” in [*Advances in Optical and Mechanical Technologies for Telescopes and Instrumentation V*], Navarro, R. and Geyl, R., eds., **12188**, 121882I, International Society for Optics and Photonics, SPIE (2022).
- [28] Westsik, M., Wells, J. T., Chahid, Y., Morris, K., Milanova, M., Beardsley, M., Harris, M., Ward, L., Alcock, S. G., Nistea, I. T., Cottarelli, S., Tammias-Williams, S., and Atkins, C., “From design to evaluation of an additively manufactured, lightweight, deployable mirror for Earth observation,” **12677-41**, International Society for Optics and Photonics, SPIE (2023).
- [29] Schwartz, N., Brzozowski, W., Ali, Z., Milanova, M., Morris, K., Bond, C., Keogh, J., Harvey, D., Bissell, L., Sauvage, J.-F., Dumont, M., Correia, C., Rees, P., and Bruce, H., “6U CubeSat deployable telescope for optical Earth observation and astronomical optical imaging,” in [*Space Telescopes and Instrumentation 2022: Optical, Infrared, and Millimeter Wave*], Coyle, L. E., Matsuura, S., and Perrin, M. D., eds., **12180**, 1218031, International Society for Optics and Photonics, SPIE (2022).
- [30] Snell, R., Atkins, C., Schnetler, H., Chahid, Y., Beardsley, M., Harris, M., Zhang, C., Pears, R., Thomas, B., Saunders, H., Sloane, A., Maddison, G., and Todd, I., “Towards understanding and eliminating defects in additively manufactured CubeSat mirrors,” in [*Advances in Optical and Mechanical Technologies for Telescopes and Instrumentation V*], Navarro, R. and Geyl, R., eds., **12188**, 121880V, International Society for Optics and Photonics, SPIE (2022).
- [31] Hafenstein, S., Hitzler, L., Sert, E., Öchsner, A., Merkel, M., and Werner, E., “Hot isostatic pressing of aluminum–silicon alloys fabricated by laser powder-bed fusion,” *Technologies* **8**(3) (2020).
- [32] Tammias-Williams, S., Withers, P., Todd, I., and Prangnell, P., “Porosity regrowth during heat treatment of hot isostatically pressed additively manufactured titanium components,” *Scripta Materialia* **122**, 72–76 (2016).
- [33] Ramola, M., Yadav, V., and Jain, R., “On the adoption of additive manufacturing in healthcare: a literature review,” *Journal of Manufacturing Technology Management* **30**, 48–69 (2019).
- [34] Blakey-Milner, B., Gradl, P., Snedden, G., Brooks, M., Pitot, J., Lopez, E., Leary, M., Berto, F., and du Plessis, A., “Metal additive manufacturing in aerospace: A review,” *Materials & Design* **209**, 110008 (2021).
- [35] Olsson, N. O., Arica, E., Woods, R., and Madrid, J. A., “Industry 4.0 in a project context: Introducing 3D printing in construction projects,” *Project Leadership and Society* **2**, 100033 (2021).
- [36] National Academies of Sciences, Engineering, and Medicine, [*Pathways to Discovery in Astronomy and Astrophysics for the 2020s: Highlights of a Decadal Survey*], The National Academies Press, Washington, DC (2023).